Electronic Supplementary Information (ESI)

Lamellar $MoSe_2$ Nanosheets Embedded with MoO_2 Nanoparticles: Novel Hybrid Nanostructures Promoted Excellent Performances for Lithium Ion Batteries

Xu Zhao, [a, b] Jiehe Sui, [a*] Fei Li, [a] Haitao Fang, [a] Hongen Wang, [b] Jiangyu Li, [c] Wei Cai, [a] Guozhong Cao [b*]

[a] *School of Materials Science and Engineering, Harbin Institute of Technology, Harbin, 150001, China*

[b] *Department of Materials Science and Engineering, University of Washington, Seattle, WA 98195, USA*

[c] *Department of Mechanical Engineering, University of Washington, Seattle, WA 98195, USA*

*To whom correspondence should be addressed:

suijiehe@hit.edu.cn;

gzcao@u.washington.edu

Discussion on weight ratios in three MoO_2@$MoSe_2$ heterostructures

Assuming that all $MoSe_2$ in first hydrothermal reaction was used to be loaded in the second step (1 mmol $MoSe_2$, about 0.254 g). From XRD patterns listed in Figure 1 and Figure S1, we cannot distinguish MoO_3 peaks, which indicate that raw materials are reduced to MoO_2 thoroughly. Considering ethylene glycol (EG) is can be a reduction reagent in many reported papers, thus he redox reaction from MoO_3 to MoO_2 in EG could possibly be ascribe to:

$$HO\text{-}CH_2\text{-}CH_2\text{-}OH + MoO_3 \xrightarrow{200\,^{\circ}C\ 24\ h} O{=}CH_2\text{-}CH_2{=}O + MoO_2 + H_2O$$

Take 0.1 g MoO_3 as an example, the theoretical yield of MoO_2 is about 0.089 g. So the weight ratio of MoO_2

to $MoSe_2$ is 0.35:1. Similarly, when we use 0.05 g MoO_3 and 0.2 g MoO_3, the weight ratios of MoO_2 to $MoSe_2$ are 0.175:1and 0.7:1, respectively.

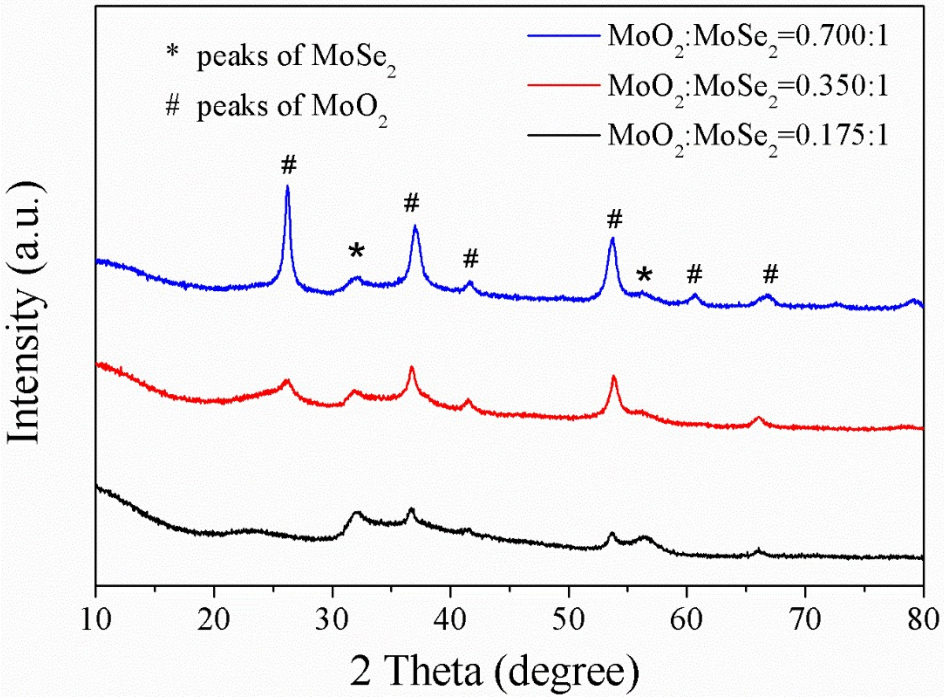

Figure S1. XRD patterns of MoO_2@$MoSe_2$ heterostructures with different mass ratios.

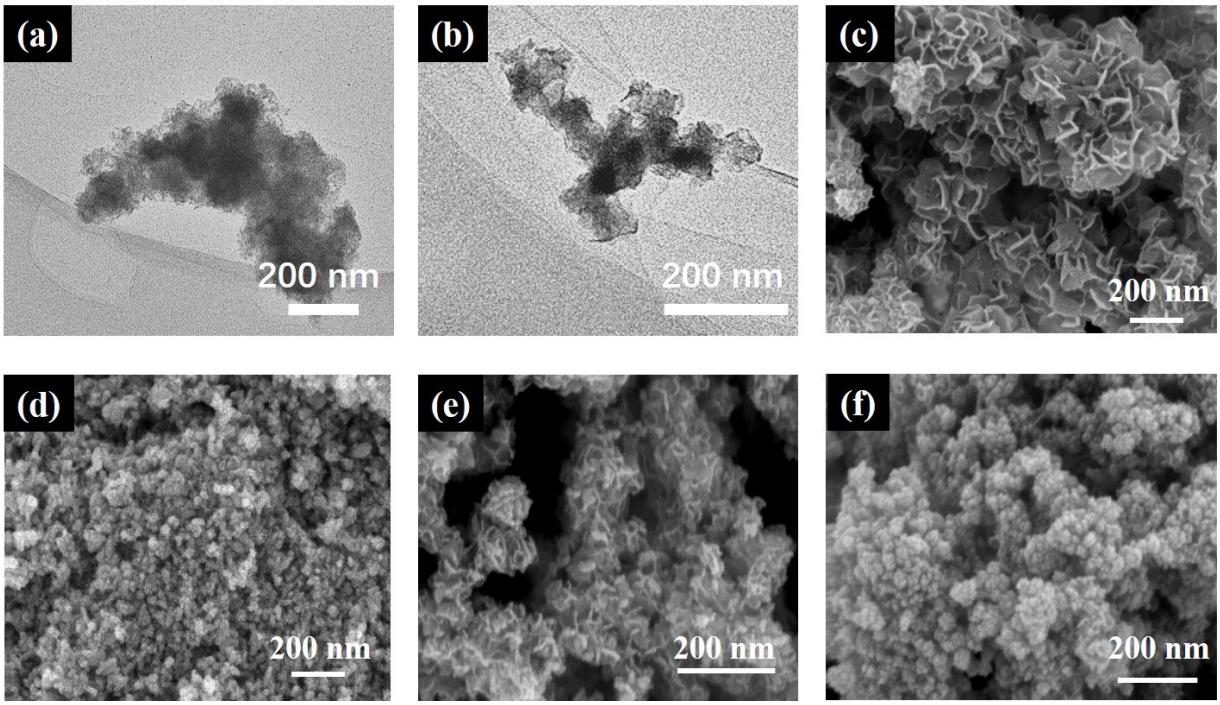

Figure S2. Low magnification TEM results of (a) bare $MoSe_2$ and (b) 2-MoO_2@$MoSe_2$ heterostructure; SEM results of (c) Bare $MoSe_2$ experienced a second solvothermal process without loading MoO_2; (d) bare MoO_2, (e) 1-MoO_2@$MoSe_2$ and (f) 3-MoO_2@$MoSe_2$.

Table S1. Comparison of rate performance of samples MoO_2@$MoSe_2$, MoO_2 and $MoSe_2$

Samples	Rate performance [#] ($mAh\ g^{-1}$)								Retention Rate[##] (%)
	100 $mA\ g^{-1}$	200 $mA\ g^{-1}$	500 $mA\ g^{-1}$	800 $mA\ g^{-1}$	1000 $mA\ g^{-1}$	1500 $mA\ g^{-1}$	2000 $mA\ g^{-1}$	100 $mA\ g^{-1}$	
MoO_2@$MoSe_2$	1136	1072	970	863	776	610	485	1040	92
MoO_2	685	640	515	215	121	45	9.7	429	63
$MoSe_2$	705	746	530	307	131	87.8	4.9	510	72

Taken from the 5th cycle at each current density; ## Taken from the 45th cycle in the end.

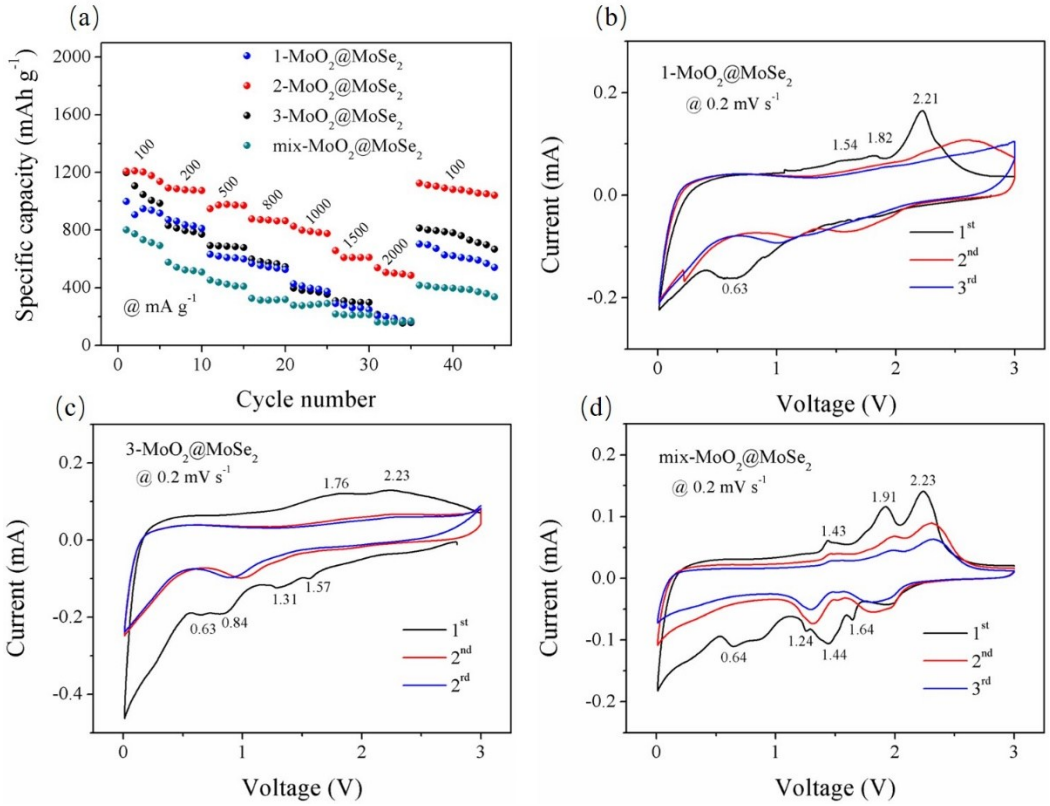

Figure S3. Rate performances of (a) MoO_2@$MoSe_2$ heterostructures with different mass ratios and mix-MoO_2@$MoSe_2$; CV results (0.2 mV s^{-1}) of (b) 1-MoO_2@$MoSe_2$; (c) 2- MoO_2@$MoSe_2$; (d) mix- MoO_2@$MoSe_2$.

Table S2. Rate performances of samples with different mass loading.

Samples*	Rate performance (mAh g^{-1}) #								Retention Rate (%) ##
	100 mA g^{-1}	200 mA g^{-1}	500 mA g^{-1}	800 mA g^{-1}	1000 mA g^{-1}	1500 mA g^{-1}	2000 mA g^{-1}	100 mA g^{-1}	
a	916	810	599	524	373	247	168	541	59
b	1136	1072	970	863	776	610	485	1040	92
c	986	770	678	544	353	297	158	666	67
d	692	506	408	319	290	211	168	336	49

* (a) 1-MoO_2@$MoSe_2$; (b) 2-MoO_2@$MoSe_2$; (c) 3-MoO_2@$MoSe_2$, (d) mix-MoO_2@$MoSe_2$, respectively. # Taken from the 5^{th} cycle at each current density; ## Taken from the ratio of 5^{th} and 45^{th} at the end.

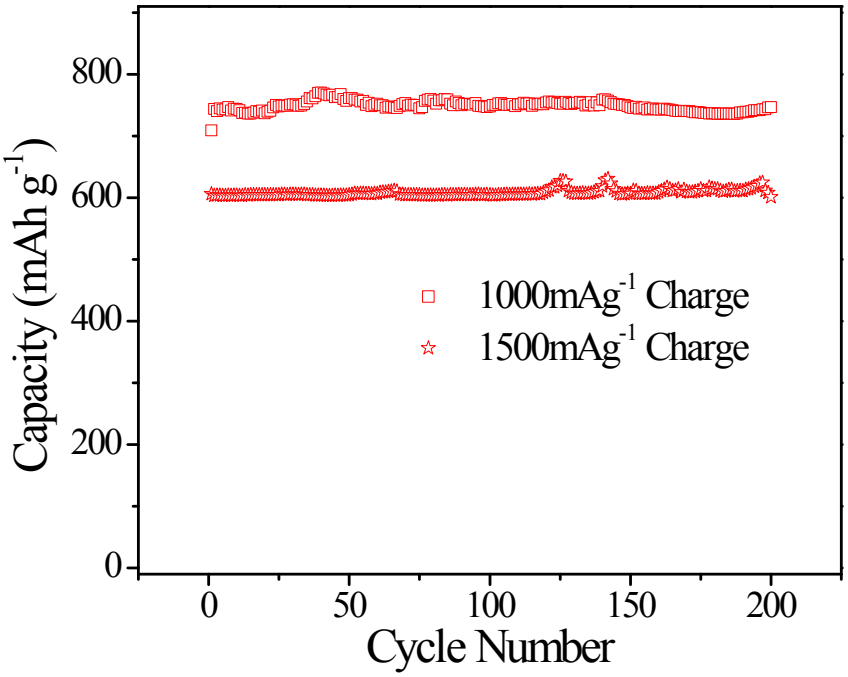

Figure S4. Cycle performance of MoO_2@$MoSe_2$ heterostructures under 1000 and 1500 mA g^{-1} current density.

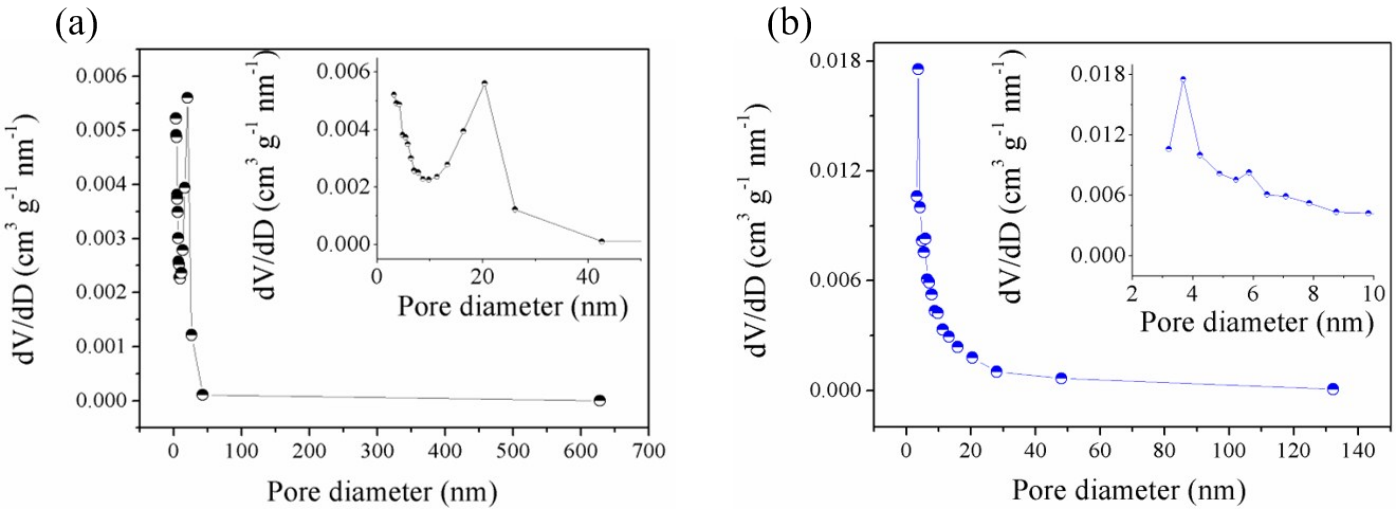

Figure S5. Pore size distribution of (a) bare MoO_2 and (b) bare $MoSe_2$